

# Technological Advancements and Manufacturing Readiness of Micro-LED Displays

Mingwei Zhu, Hou T Ng, Sivapackia Ganapathiappan, Zhiyong Li, and Nag Patibandla

Nag\_Patibandla@amat.com  
Applied Materials Inc., 3225 Oakmead Village Dr, Santa Clara, USA  
Keywords: Micro-LED, Quantum Dots, Front-Plane, Display Technology.

## ABSTRACT

Applied Materials is pursuing an innovative approach to develop micro-LED display technology that is suitable to address both direct-view and near-eye (AR/VR) applications. This approach uses high efficiency UV micro-LEDs, active-matrix backplanes with four subpixels, in-situ curing of QD formulation, simplified die-transfer, and repair scheme. In this paper, progress in the assembly of a smartwatch size display, custom-built tools, scalable processes, and key advantages is reported.

## 1 Introduction

Applied Materials, Inc (Applied) reported earlier [1] on an innovative approach on  $\mu$ LED front plane technology using a single-wavelength gallium nitride (GaN) LED emitter with Cadmium-free quantum dots (QDs) for color conversion. This proprietary  $\mu$ LED front plane technology incorporates several key innovations such as the use of high external quantum efficiency (EQE)  $\mu$ LED dice in ultraviolet (UV) wavelength spectrum (vs. red/green/blue), capable of yielding highest quantum efficiency at a small die-size (< 10 $\mu$ m), with fewer number of mass transfer steps with high yield, and a four-subpixel backplane architecture to allow for a simple, cost-effective repair strategy.

In order to validate our approach and its key advantages, Applied, together with its partners and suppliers, has fabricated a smartwatch size display (shown in Section 4.1 of this paper). In this paper, Applied's new  $\mu$ LED display architecture, its key innovations, and HVM scalable tools are discussed. The paper also provides information on key advantages of the approach with respect to simplified die mass transfer, use of subpixel for repair, improved current efficiency, and better viewing angles vs. other display types. The readiness of this technology at manufacturing scale to address various display applications in a cost-effective manner is evidently demonstrated.

## 2 Experiment

### 2.1 New micro-LED display architecture

Fig. 1 illustrates our display architecture. 385nm UV  $\mu$ LED and customized 2T1C active-matrix (AM) backplane (BP) were fabricated per our design and specifications. UV  $\mu$ LED dice were transferred to BP by mass transfer through laser liftoff, interposer transfer, and die bonding. Pixel isolation walls were built between  $\mu$ LED dice to avoid

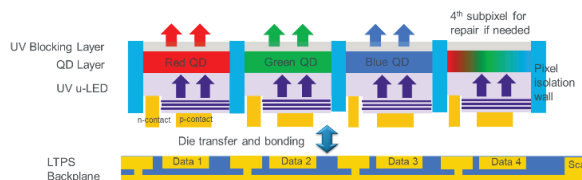


Fig. 1 Architecture of Applied Materials' novel  $\mu$ LED display

light crosstalk and provide wells for subsequent QD formulation printing. Commercial-scale, performance optimized, Cd-free R/G/B QDs were sourced from a QD materials partner. QD formulations were optimized for printability on our custom-built, high-resolution inkjet platform. In addition, the QD formulation contains photoinitiators sensitive to UV light so that it can be cured by the UV  $\mu$ LED within each subpixel via self-aligned curing. For the color conversion layer fabrication, RQDs were printed into the R subpixel first and cured by the UV  $\mu$ LED selectively turned on in R subpixels only. RQDs outside R subpixels are washed away afterwards as they are not cured. We repeat the same for G and B QDs to get the full color on BP. The 4th subpixel will be used to repair if any of the three colors/subpixel become defective. The process is then followed by encapsulation and UV blocking layer application to seal QD-layer and prevent excessive UV emission leakage from the display.

### 2.2 UV micro-LEDs

UV LED wafers with peak wavelength of 385nm were grown on 4" sapphire substrate in commercial MOCVD reactors. Flip-chip  $\mu$ LED of 30 $\mu$ m x 30 $\mu$ m were fabricated with through mesa and isolation etching, followed by sidewall dielectric passivation and metallization. Sapphire substrates were polished by chemical-mechanical polishing (CMP) to achieve optical smoothness for subsequent laser liftoff (LLO) process to separate GaN-based  $\mu$ LED from its growth substrate.

By adopting a patterned sapphire substrate (PSS), we have successfully improved the EQE of 30 $\mu$ m x 30 $\mu$ m UV  $\mu$ LED from 24% to 36%), attributed to the enhancement of both internal quantum efficiency (IQE) and light extraction efficiency (LEE). We believe such EQE is close to the EQE of blue  $\mu$ LED of similar die size.

### 2.3 Cadmium-free RGB QDs and Inkjet Printing

QD-based displays have gained increasing market share over the past few years [2]. In the approach used here, Cd-free QDs emitting all three primary colors, R/G/B, optimized for activation at 385nm UV wavelength are used. The QDs are formulated into ink-jettable and UV-curable formulations in acrylic monomer medium, followed by an inkjet process which accurately prints QDs in specific sub-pixels. The formulation requires a unique set of monomers (compatibility to QDs) and additives (stabilizing agents and to control surface tension) along with non-yellowing photoinitiators so that QDs are well dispersed and maintain their dispersion stability for a long time. It is well known that blue QD is the hardest one to synthesize [3] due to its smaller size (that could increase the reactivity with increase in surface area) with the correct bandgap. Good progress has been made in EL blue QD [4] [5]. In this work, we focused on PL QDs. QDs require proper ligands attached to the surface for the specific acrylic medium so that they can remain dispersed. We have ensured that all the QDs are reasonably stable by improving the formulation additives and handling process along with good encapsulation followed by curing. Another key parameter is viscosity. The viscosity of the formulations is adjusted in the range suitable for ink jetting at a desired temperature with stable print performance. Composition of the ink is adjusted for each color so as to ensure stability and shelf-life. All these inks have good printability with excellent jetting dynamics such that the ink-drops can be placed accurately into the targeted subpixel wells. For various pixels/inch (ppi) settings, the drop weight can be adjusted accordingly to meter the fill volume.

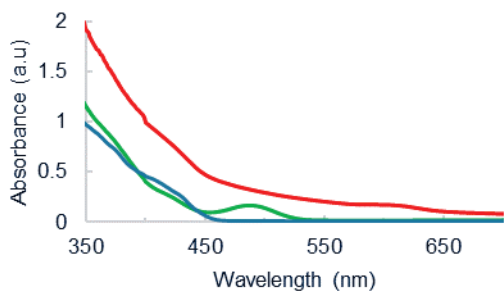


Fig. 2 UV-Vis Absorbance of RGB QDs

Absorption spectra of the RGB QDs are shown in Fig. 2. Absorption of QDs at 385 nm is roughly 3 to 5 times higher compared to that at 450 nm, indicating that this higher absorbance results in lower blue light leakage. In general, absorption of red QD is much higher than either green or blue and our formulation contains >20% of QDs to maintain desired optical requirements. Other properties of QDs such as photoluminescent quantum yield (PLQY), peak wavelength (PWL) and full width at half-maximum (FWHM) are summarized in Table 1. This clearly indicates that all our QDs have higher PLQY with narrow FWHM characteristics.

Table 1. Properties of QDs in ink-jettable formulation

QD	PLQY % (after SAC)	PWL (nm)	FWHM (nm)
Red	92	638	41.0
Green	90	518	39.5
Blue	87	453	33.0

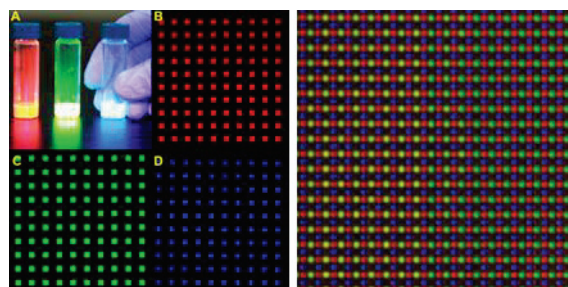


Fig. 3 (A) RGB QD inks in vials with 385nm excitation; B-D) PL of RGB QDs in pixels after inkjet printing (Left); PL of fully printed pixel layout (Right)

As shown in Fig. 3, RGB QD formulations showed strong photoluminescence (PL) and after ink-jetting into subpixels while the luminescent intensity is maintained. The lifetime of cured QD formulations, shown in Fig. 4, is measured with exposure to 385nm UV flux (>5X flux used in the actual displays) at an elevated temperature (>36°C). The matrix that we use is resistant to UV such that QD degradation is reduced significantly. Excitation UV is almost absorbed (>90%) by QDs by controlling the amount of QDs in each subpixel. The small amount of unabsorbed UV is completely filtered by encapsulating with UV blocking layer.

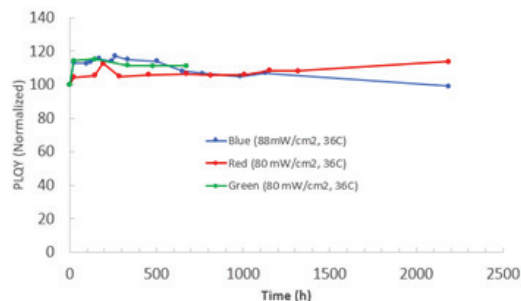


Fig. 4 Lifetime and PLQY data for Cd-free QDs (Green QD sample measurement in progress).

### 3 HVM Platforms

#### 3.1 High-Throughput Excimer Laser Tool

As discussed in [6], the commercial success of  $\mu$ LED displays is dependent on the improvement of the die-mass transfer processes and their yields. It is difficult for current mass transfer technology to achieve high-efficiency and high-precision transfer, which has aggravated the production costs. The process of mass transfer begins with  $\mu$ LED dice being separated from sapphire by a UV laser lift-off, followed by steps involving transfers onto one or two interposers made of adhesive materials such as polydimethylsiloxane (PDMS) and then transfer onto backplane and electrically bonded in-place. A HVM tool that can handle die transfer from epi substrate with

high yield is one of the most difficult challenges that  $\mu$ LED display technology is facing today. Applied has developed novel die transfer technology and a tool that can address small die transfer with high precision and yield needed for direct-view displays. As depicted in Fig. 5, our custom-built tool allows both massively parallel laser-lift off (LLO) and selective laser-induced forward transfer (LIFT) die transfer to be accomplished. High precision laser optics and mechanical motion control technologies are employed in our tool. High mass transfer rate ( $> 100\text{M}$  die UPH) and yields ( $> 5\text{N}$ ) can be realized. The bonding metallurgy between  $\mu$ LEDs and backplane was carefully optimized to achieve high electrical yield through HVM-scale bonding tools.

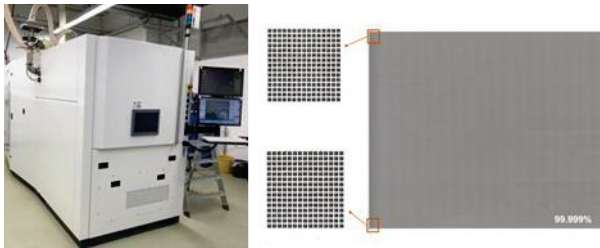


Fig. 5 Custom-built laser tool for die mass transfer (Left). Optical images show representative high yield mass transfer of  $\mu$ LEDs onto an interposer (Right)

### 3.2 High-resolution Ink-jetting Printer

Current state-of-the-art industrial printers do not provide the desired print yield, drop placement accuracy, high ppi printing, subpixel-level UV curing, and process defect control. A key innovation in the Applied approach to overcome the afore-mentioned challenges is to employ piezo-based inkjet printing to deposit QD inks onto the UV  $\mu$ LED array with the desired throughput, followed by selective self-aligned UV curing via turning on the UV LED dice to fully cure the formulation in the targeted subpixels.

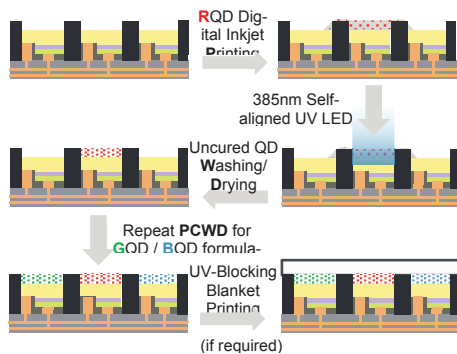


Fig. 6. PCWD process flow. Thin-film passivation can be performed after RGB QD ink-jetting, as required for device.

Fig. 6 shows our novel PCWD (printing-curing-washing-drying) process flow to deposit and selectively cure RGB QDs in targeted subpixel wells of a display panel. First, we inkjet QD inks (e.g., Red QDs) into the targeted R subpixel well array. This is followed by turning on UV  $\mu$ LEDs in each R subpixel wells to enable self-aligned bottom-up curing. An advantage of our curing strategy is that

any potential ink spillover into neighboring wells will not be cured and can be effectively removed via washing in the next immediate step, thereby eliminating display color bleed while retaining the desired CIE map during display operation. After a drying step, the substrate is ready for the next round of PCWD process. This process is repeated until all RGB subpixel wells are filled with respective cured QD inks.

We anticipate our differentiated approach to be scalable to handle various high ppi display resolutions. To ensure high print yield, onboard metrology is employed to derive a print rework lookup table (e.g., missing empty wells, partially filled wells) for respective color QDs.

Fig. 7 illustrates high uniformity in drop volume control which leads to highly consistent photoluminescence intensity of RGB QDs. Fig. 8 shows our custom-built HVM scalable high precision inkjet printer.

Fig. 7. Photoluminescence maps of ink-jetted RGB QDs and their respective intensity profiles.

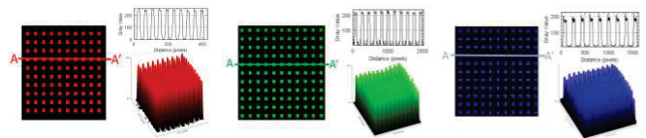
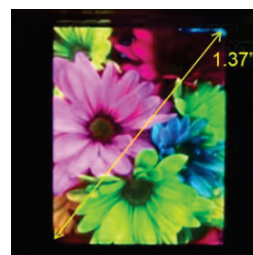


Fig. 8. HVM printer for conducting key PCWD process steps.

## 4 Results and Discussion

### 4.1 Direct-view watch demo display



Display size	1.37"
Resolution	340 x 272 (5:4)
Pixel size	80 $\mu\text{m}$ (318 ppi)
$\mu$ -LED size	30 $\mu\text{m}$ x 30 $\mu\text{m}$
TFT backplane	LTFS
Brightness	$> 1,000$ nits
Contrast ratio	$> 7,000,000$
Color gamut	$> 95\%$ DCI-P3

Fig. 9 Picture and key specs of smartwatch size  $\mu$ LED display

Fig. 9 illustrates the 1.37" demo watch display fabricated by our UV  $\mu$ LED and R/G/B QD technology on LTFS active-matrix backplane. The display pixel size is 80 $\mu\text{m}$  with ppi of 318. Brightness  $> 1,000$  nits with very high contrast ratio of  $> 7,000,000$  were achieved. We also achieved wide color gamut covering  $> 95\%$  DCI-P3.

## 4.2 Advantages of our approach

### 4.2.1 High yield from one-step mass transfer and on-demand repair from 4<sup>th</sup> subpixel

One top challenge for  $\mu$ LED display is pixel-level yield since human eye is very sensitive to display defect. For native R/G/B LED approach, since the subpixel is the  $\mu$ LED itself, each failed  $\mu$ LED die will lead to a dead subpixel so it needs to be removed and repaired. This will incur additional repair cost and impose difficulty for high PPI displays. For the display architecture we proposed, since we have four  $\mu$ LED dice in each subpixel, we will use the 4<sup>th</sup> subpixel to do repair by printing QD of missing color into the 4<sup>th</sup> subpixel if any of three subpixel fails. We only need to do die repair only when there are two or more  $\mu$ LED failure in each pixel. By adopting the 4<sup>th</sup> subpixel architecture, we expect it would greatly reduce the need for die-level repair. Fig. 10 illustrates an example with a 340 x 272 pixel display with  $\mu$ LED light up yield of 99.7%. Based on the pixel map and yield analysis, it would require 1024 physical die-level repairs for a native R/G/B LED approach instead of 8 die repairs by adopting our 4<sup>th</sup> pixel approach. Therefore, our approach would have much higher pixel yield and much reduced manufacturing cost.

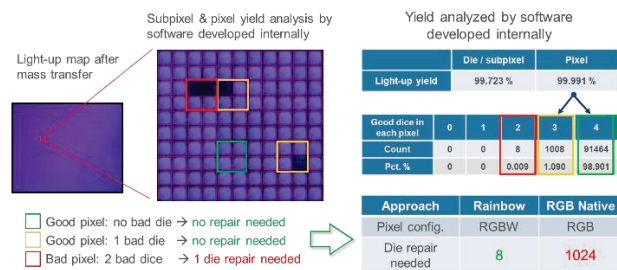


Fig.10 Die-repair reduced by the 4<sup>th</sup> pixel redundancy.

While a native RGB approach would require mass transferring  $\mu$ LED dice from three separate source wafers with difference wavelengths to the backplane, we will need to do a transfer from one UV-A source wafer. It would reduce the complexity for mass transfer as it involves fewer steps for movement. Since our display colors are from QDs not from the  $\mu$ LED, we can also tolerate wide wavelength distribution from UV  $\mu$ LEDs as QDs can be pumped from a wide range of UV wavelength. Therefore, we can achieve higher wafer utilization than the native R/G/B approach which requires very high wavelength of 1-2nm across the transfer area [8].

### 4.2.2 Better Efficiency and Better Viewing Angle

As display needs R/G/B light to achieve white light, good efficiency from all primary colors is required. Blue organic emitter has a fundamental material challenge in efficiency and lifetime from its fluorescent emission, resulting in a limited performance for Organic LED (OLED) [8]. For native RGB LED approach, efficiency of red  $\mu$ LED, either from AlGaInP or InGaN material is far behind its counterpart blue and green emitters, due to excessive carrier loss

at sidewall or in defective QWs [9]. Our approach of using R/G/B QDs balances the efficiency for three colors therefore we can achieve higher white light efficiency over OLED or native RGB  $\mu$ LED.

We have also collected the light emission pattern of our display from 0 to 70 degrees. It shows good uniformity in both color and intensity. This agrees with the Lambertian emission pattern for color conversion QD from optical modeling by LightTools. This shows another advantage over the native R/G/B LED approach where mismatched angular distributions were observed between AlGaInP-based red and InGaN-based blue/green counterparts due to refractive index difference [10]

## 5 Conclusions

In this paper, an innovative and HVM-scalable approach to fabricate full-color  $\mu$ LEDs display using active matrix TFT backplanes with four subpixels, high efficiency UV  $\mu$ LEDs and in-situ curing of Cd-free R/G/B QD formulations was discussed. A simplified die-transfer and much reduced die repair scheme with 4<sup>th</sup> subpixel were developed and demonstrated. We reported our progress in assembling a smartwatch size display based on the approach described above and have showed its superior performance in efficiency and viewing angle over other  $\mu$ LED approaches. The readiness of manufacturing tools, materials and processes were also discussed. The architecture of UV  $\mu$ LED with QD color conversion has shown potential for augmented/virtual reality (AR/VR) display applications, where extremely high brightness, full color at high resolution >3000 ppi are required. Development of a full-color UV  $\mu$ LED and QD color conversion layer integrated on a CMOS backplane using semiconductor fabrication processes is in progress.

## 6 References

- [1] N. Patibandla, 2021 Virtual Display Week International Symposium, May 17-21 (2021).
- [2] P. Palomaki, Seminar SE-3 in SID International Symposium, May 8-13 (2022)
- [3] S. Chen, et al., Nat. Commun., 10, 765 (2019).
- [4] T. Kim, et al. Nature, 586, 385–389 (2020).
- [5] S. H. Lee, et al. Chemistry of Materials, 32 (13), 5768-5775 (2020).
- [6] Y Wu, et al. Nanomaterials, Nanomaterials, 10(12), 2482 (2020).
- [7] A. Paranjpe, et al., SID Symposium Digest of Technical Papers. Vol. 49 Issue 1, p597-600 (2018).
- [8] SW Wen, et al., Journal of display technology, Vol 1 (1), pp. 90-99 (2005)
- [9] T.K Oh, et al., Opt. Express Vol. 26, Issue 9, pp. 11194-11200 (2018).
- [10] F. Gou, et al. Opt. Express Vol. 27, Issue 12, pp. A746-A757 (2019).